SECED 2015 Conference: Earthquake Risk and Engineering towards a Resilient World
9-10 July 2015, Cambridge UK

RISK-BASED SEISMIC PERFORMANCE ASSESSMENT OF EXISTING TALL STEEL-FRAMED BUILDINGS IN SAN FRANCISCO

Carlos MOLINA HUTT[1], Gregory DEIERLEIN[2], Ibbi ALMUFTI[3] and Michael WILLFORD[4]

ABSTRACT

This study presents the results of a risk-based seismic performance assessment of an archetype tall building representative of the existing tall building stock in San Francisco, CA. The archetype tall building, selected based on an inventory of existing tall buildings, is a 40-storey Moment Resisting Frame (MRF) representative of design and construction practice from the 1970-s to the mid-1980s. A Multiple Stripe Analysis (MSA) was conducted at 8 different intensity levels ranging from frequent to very rare seismic events, i.e. from 85% to 1% probability of exceedance in 50 years. Non-Linear Response History Analyses (NLRHA) were conducted with ground motions representative of each intensity level considered. The results of the NLRHA results were used to assess the probability of earthquake losses, considering collapse potential and the probability of the building deemed irreparable due to permanent residual drifts in the structure.

Based on the MSA results, the collapse fragility of the structure, assumed to follow a lognormal cumulative distribution expressed as a function of spectral acceleration at the fundamental period of the structure (T=5 seconds), has an estimated median of 0.15g and a dispersion of 0.30. A number of loss metrics were developed for the archetype building including: a loss function, which provides the annual frequency of exceeding a certain value of loss, e.g. the expected 500 year loss equals $53M or 39% of the building replacement cost; the expected Average Annual Loss (AAL) equal to $0.6M or 0.46% of the building replacement cost; and loss exceedance rates, e.g. a loss of 10% building replacement cost or $13.5M has an exceedance rate of 95 years. The use of these results to benchmark the performance of the archetype tall building against the design intent in current building codes and to assess the impact of structural retrofit or other building enhancements is discussed.

MOTIVATION

Tall buildings play an important role in the socio-economic activity of major metropolitan areas in the United States. The resilience of these structures is critical to ensure a successful recovery after major disasters. Until the introduction of Performance Based Seismic Design (PBSD) in the 1990s, tall buildings were designed using conventional building code guidelines (FEMA 2006) which do not provide an explicit understanding of performance during major earthquakes. Researchers and engineers have raised concerns that the prescriptive approach of building codes is not suitable for tall building design due to the significant contribution of higher mode effects (PEER 2010). As a result of these shortcomings, several jurisdictions in areas of high seismicity throughout the Unites States (e.g. Los Angeles and San Francisco) have adopted a PBSD approach for the design of new tall buildings. While new designs follow a more adequate approach, little is known about the seismic performance of older existing tall buildings that were designed prior to the adoption of PBSD (Molina Hutt et al. 2014).

The goal of this work is to benchmark the performance of existing tall buildings that were designed prior to the implementation of PBSD guidelines. In order to influence decision making, results are expressed as the expected consequences in terms of direct economic losses and are developed to enable cost-benefit analyses of potential structural and non-structural enhancements that could increase the seismic resilience of these buildings.

[1] Teaching Fellow, University College London, London, UK. Email: carlos.molinahutt@ucl.ac.uk
[2] Professor, Stanford University, Stanford, CA, USA. Email: ggd@stanford.edu
[3] Associate, Arup, San Francisco, CA, USA. Email: ibrahim.almufti@arup.com
[4] Principal, Arup, San Francisco, CA, USA. Email: michael.willford@arup.com

METHODOLOGY

This paper presents a risk-based seismic performance assessment of an archetype tall building for a case study city, San Francisco. A risk-based seismic assessment provides information on expected performance of a building over a specified time horizon. This time-based performance assessment is more comprehensive than scenario-based or intensity-based assessments, which evaluate building performance under either a scenario earthquake event or a specified intensity of ground shaking, respectively. A risk-based assessment consists of the evaluation of a number of intensity-based performance assessments under a range of ground motion intensity levels which are then combined with the ground motion hazard curve, as illustrated in Figure 1, to provide the annual rates of exceedance of a performance measure, e.g. losses (NEHRP 2011).

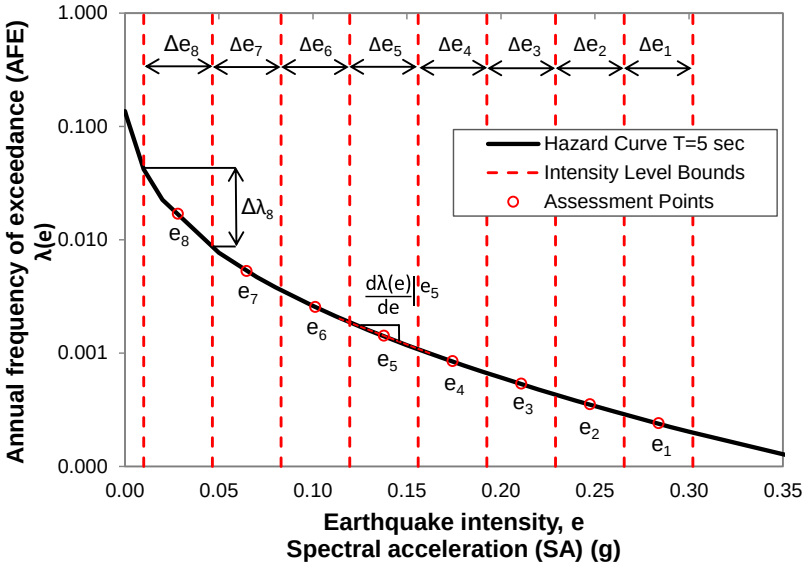

Figure 1. Seismic hazard curve at site of interest in downtown San Francisco (V_{s30}=260m/s, T=5sec.) illustrating the earthquake ground motion intensities (e_i) considered in the risk-based assessment.

The technical basis of the methodology followed to conduct the risk-based seismic performance assessment is that developed by the Pacific Earthquake Engineering Research (PEER) Centre, which applies the total probability theorem to predict earthquake consequences in terms of the probability of incurring a particular value of a performance measure (Moehle and Deierlein, 2004). Under this framework, performance is computed by integrating: the probability of incurring an earthquake of different intensities over all possible intensities; the probability of incurring a certain building response (drift, acceleration, etc.) given an intensity of ground shaking; and the probability of incurring certain damage and consequences given a value of building response (FEMA 2012). The implementation of such methodology to assess the performance of the archetype tall steel-framed building in San Francisco can be broken into the following steps:

-Archetype Building and Representative Site Selection
-Structural Analysis Modelling
-Seismic Hazard and Ground Motion Selection
-Building Performance Modelling

Archetype Building and Representative Site Selection

The Structural Engineers Association of Northern California (SEAONC) Committee on PBSD of Tall Buildings developed an inventory of the existing tall building stock in San Francisco. This committee identified more than 90 buildings of 20 stories or greater, most of which employed a steel moment frame lateral system (Molina Hutt et al. 2014). Based on building characteristics such as location, height, number of stories, year of construction and lateral

resisting system type, a 40-storey steel MRF designed per the 1973 Uniform Building Code was selected as the archetype building for this study. A representative site was selected in close proximity to many of the existing tall buildings in downtown San Francisco with soil properties consistent with ASCE 7-10 Site Class D (ASCE 2010). Detailed information on the existing tall building database, the selection of the archetype building, the site selection and the design process can be found in Molina Hutt et al. (2014).

Structural Analysis Modelling

The structural analysis model was developed in LS-DYNA (2013) to include non-linear columns, beams, panel zones and column splices. Concrete slabs were modelled as elastic cracked concrete 2D shell elements to represent the floor diaphragm. Columns and beams were modelled as lumped plasticity beam elements. Columns captured bi-axial bending moment and axial force interaction as well as buckling in compression. Beams included a random fracture model to determine the plastic rotation at which fracture occurs in moment connections based on field observations and test data developed following the 1994 Northridge earthquake. Panel zones were modelled by an assembly of rigid links and rotational springs. Column splices were modelled as non-linear springs capable of reaching the nominal capacity of the connection followed by a brittle failure as observed in experiments. Detailed information on the structural analysis model development and its non-linear components can be found in Molina Hutt (2013).

Seismic Hazard and Ground Motion Selection

Structural analysis was performed at a series of ground motion intensities spanning from low to high probability of occurrence. The minimum and maximum annual frequencies of exceedance (AFE) and corresponding spectral accelerations (SA) at the fundamental period of the structure considered in the assessment were as follows:

- Minimum: AFE corresponding to SA_{MIN} = 0.05g/T where T is the fundamental period
- Maximum: AFE = 0.0002 and corresponding SA_{MAX}

The upper and lower bound intensity levels were considered in this study based on the recommendation of FEMA (2012) to cover a range from negligible damage to complete loss. These bounds were obtained from the seismic hazard curve at the fundamental period of the structure, as shown in Figure 1. The lower bound should correspond to a ground motion intensity level that does not result in significant damage to structural or non-structural components whereas the upper bound should correspond with a ground motion intensity no more than two intensities of shaking beyond the level that triggers collapse.

Once the bounds of spectral accelerations SA_{MIN} to SA_{MAX} at the fundamental period of the structure were determined, the range was split into a number of equal intervals for assessment. Based on the recommendation of FEMA (2012), 8 intensity level intervals were selected to capture a wide range of responses. The midpoint SA of each one of these intervals was then computed and its corresponding AFE. This process is graphically illustrated in Figure 1, where the earthquake ground motion intensity intervals and the assessment points are denoted by Δe_i and e_i respectively. The AFE and SA associated with each earthquake ground motion intensity level considered in the assessment are summarized in Table 1.

Table 1. SAs, AFEs and associated return periods for the ground motion intensities considered.

Earthquake Ground Motion Intensity	SA (g)	λ(e) (AFE)	Return Period (years)
e_1	0.284	0.00024	4156
e_2	0.247	0.00035	2833
e_3	0.211	0.00054	1861
e_4	0.174	0.00085	1177
e_5	0.138	0.00143	702
e_6	0.101	0.00255	392
e_7	0.065	0.00549	182
e_8	0.028	0.01850	54

Uniform Hazard Spectrum (UHS) was selected as the target spectrum for each of the intensity levels considered in the assessment, as shown in Figures 2a through h. For each intensity level, 11 ground motion pairs were selected in order to provide a reasonable estimate of the median response. Previous studies suggest that when the spectral shape of the selected motions matches the target spectrum well, relatively few records can provide a reasonable estimate of median response over the height of the building (FEMA 2012).

In order to select ground motions to match the target spectra, the NGA West 2 Ground Motion Database was used for record selection (PEER 2013). A wide range of record characteristics (fault type, magnitude range, etc.) were used to search the database such that the computed mean squared error of the geomean spectrum of the records (5% damping) and the suite average was minimized with respect to the target spectrum over the period range of interest of the structure spanning from 0.2T to 1.5T (ASCE 2010), where T is the fundamental period. Only linearly scaled ground motions were selected in order to maintain record to record variability i.e. the frequency content of the selected earthquake records was not altered through response-spectrum matching.

The effect of ground motion pulses and soil structure interaction were not explicitly considered in the analyses. The selected ground motions were input at the base of the structural model, which was assumed to have a rigid base at the top of the foundation.

Building Performance Modelling

The building performance is evaluated in this study in terms of the probability of earthquake damage and losses, where the costs are expressed in present dollars. Losses are expressed in terms of normalized repair costs, i.e. the cost required to restore a building to its pre-earthquake condition, normalized by the total building replacement value, i.e. the cost required to rebuild with a new structure of similar construction. The replacement cost for the archetype tall building is estimated to be $330 per square foot in present US dollars (Molina Hutt et al. 2014).

The building performance model contains structural and non-structural components at each story level for all components in the building that are susceptible to earthquake damage. Structural component quantities are based on the structural design of the archetype building. Non-structural component quantities are estimated based on typical quantities found in buildings of similar occupancy by use of the Normative Quantity Estimation Tool (FEMA 2012).

Engineering demand parameters (EDP) evaluated in the NLRHA analyses include maximum interstory drift ratios (IDR) and peak floor accelerations, which were determined at every story in the building for each intensity level considered in the assessment. Figure 3 illustrates the input EDPs to the building performance model obtained from the NLRHA results for intensity levels e_5 through e_8. Results for intensity levels e_1 through e_4 are not shown because a large number of analysis runs induce collapse at these higher intensities of shaking. The implications of collapse in the loss assessment are discussed later in the results section.

Loss estimates for the non-collapse cases were conducted using the FEMA P-58 Performance Assessment Calculation Tool (PACT) (FEMA 2012). The probability of residual drifts rendering the building irreparable were also calculated using PACT assuming typical building repair fragility as a function of residual drifts is a lognormal distribution with a median value of 1% residual drift ratio and a dispersion of 0.3 (FEMA 2012).

Detailed information on the development of the building performance model such as the structural and non-structural building components, their fragilities and consequence functions can be found in Molina Hutt et al. (2014).

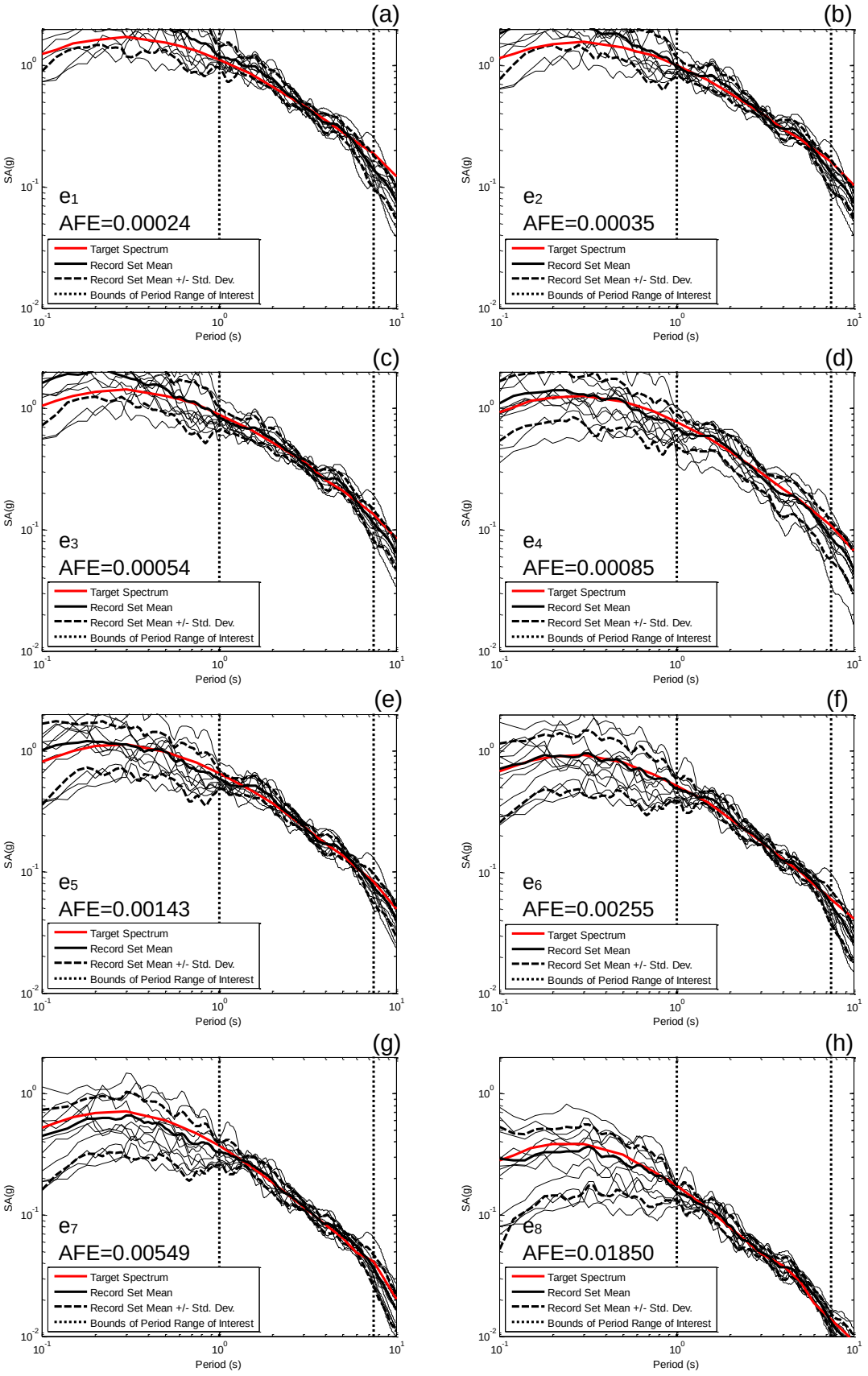

Figure 2. Target spectrum and individual ground motion spectra for intensity levels e_1 to e_8 (a through h).

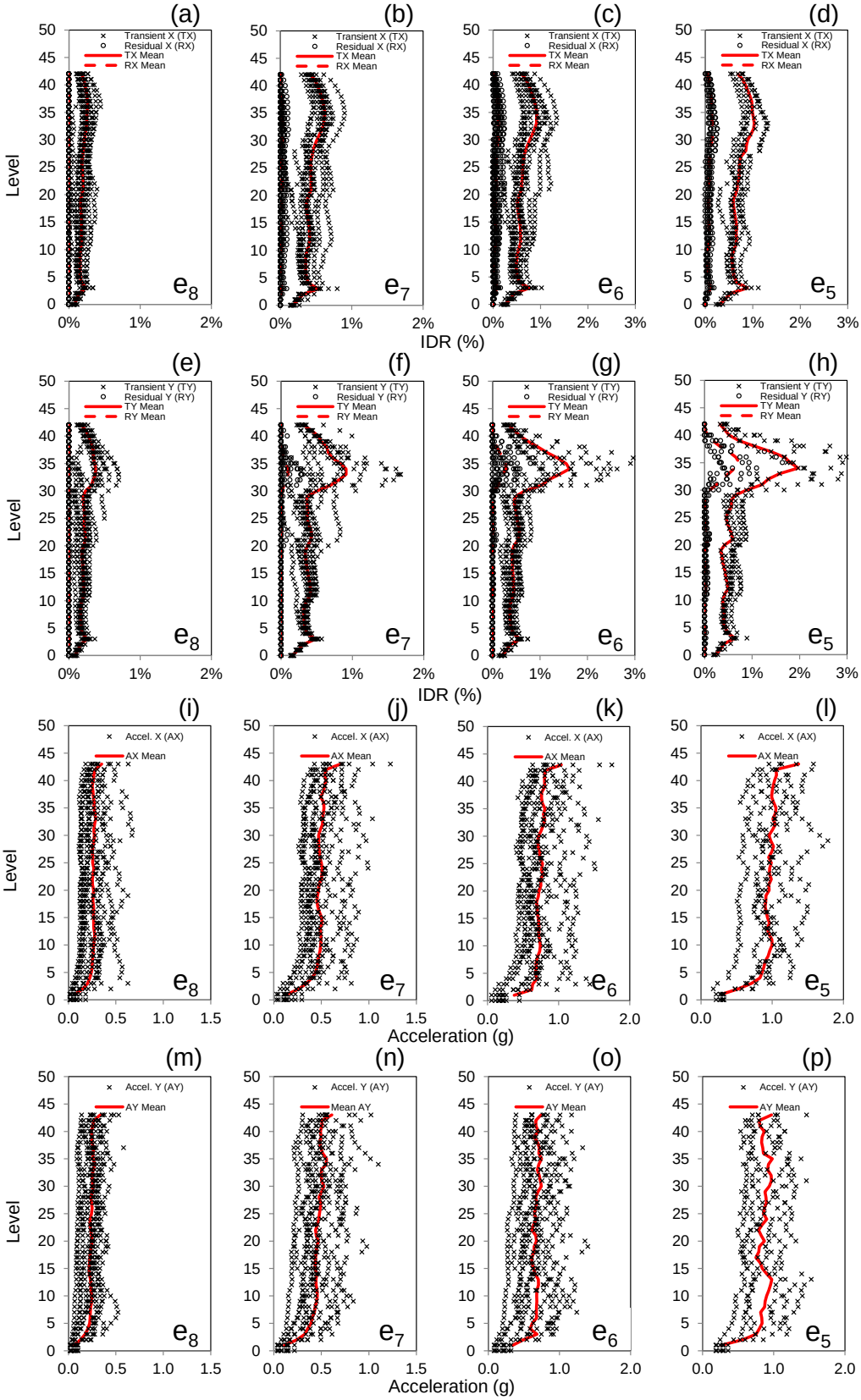

Figure 3. EDPs used as input into the building performance model: transient and residual IDRs in X (a-d) & Y (e-h) and accelerations in X (i-l) & Y (m-p) for intensity levels e_5 to e_8.

RESULTS

The results of the MSA were used to develop the collapse fragility for the archetype building and the associated loss function, which provides the annual frequency of exceeding a certain value of loss and enables the calculation of other loss metrics. These results are used to (1) benchmark performance against the design intent in current building codes, (2) communicate performance to decision makers, and (3) assess the impact of structural retrofit or other building enhancements.

Collapse Fragility and Annual Rate of Collapse $\lambda_{Collapse}$

This study followed a MSA approach in which NLRHA were performed at 8 intensity levels and where different ground motions were used at each intensity level under consideration as discussed earlier. At the higher earthquake ground motion intensities, the fraction of ground motions that cause structural collapse are recorded and used to obtain the collapse fragility for the building. The statistical fitting technique for this data follows the method of maximum likelihood as described by Baker (2015).

The MSA results are illustrated in Figure 4b, which illustrate in the vertical axes the target SA for the intensity level considered against the peak IDR in each analysis run. The results shown beyond the 6% IDR mark denote collapse runs and are offset to ease visualization. The resulting collapse fragility has an estimated median of 0.15g and a dispersion of 0.30 as illustrated in Figure 4a.

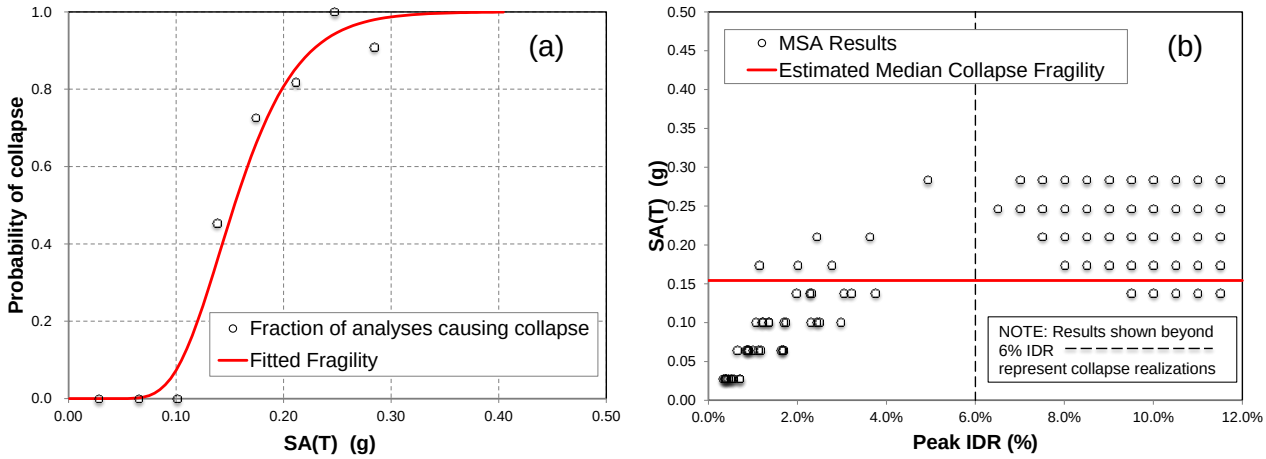

Figure 4. Collapse fragility (a) derived from MSA results (b).

The collapse fragility function is then used to estimate the annual rate of collapse of the structure, $\lambda_{Collapse}$, by integrating with the hazard curve as illustrated in Equation 1 (Baker 2015, Medina and Krawinkler 2003):

$$\lambda_{Collapse} = \int \mathrm{P(C|E = e)}\,|\mathrm{d\lambda(e)}| \qquad (1)$$

This term $\mathrm{P(C|E = e)}$, the probability of observing collapse at a given intensity level as denoted by the collapse fragility illustrated in Figure 4, is integrated with the seismic hazard curve, $|\mathrm{d\lambda(e)}|$, as illustrated in Figure 1. Solving Equation 1 by numerical integration yields an expected annual probability of collapse for the archetype tall building of 0.0015. If we assume the occurrence of collapse follows a Poisson process, the probability of collapse in a specified time horizon, *t*, can then be estimated per Equation 2 (Baker 2015, Ibarra and Krawinkler 2005, Medina and Krawinkler 2003):

$$P_{Collapse} = 1 - e^{-\lambda_{Collapse} \cdot t} \qquad (2)$$

Loss Function and Expected Average Annual Loss (AAL)

The loss function provides the annual frequency of exceeding a certain value of loss and can be calculated using Equation 3 (FEMA 2012, Krawinkler and Miranda 2004, Goulet et al. 2007):

$$P(L > x) = \int P(L > x|E = e)\ |\mathrm{d}\lambda(\mathrm{e})| \tag{3}$$

where $P(L > x|E = e)$, the probability of exceeding a certain value of loss at a given intensity, is integrated with the seismic hazard curve, $|\mathrm{d}\lambda(\mathrm{e})|$, as illustrated in Figure 1. The $P(L > x|E = e)$ can be broken down as the sum of three components:

- $P(L > x|C) \cdot P(C|E = e)$
- $P(L > x|NC, R) \cdot P(NC|E = e) \cdot P(R|NC, E = e)$
- $P(L > x|NC, NR) \cdot P(NC|E = e) \cdot P(NR|NC, E = e)$

Component $P(L > x|C) \cdot P(C|E = e)$ denotes the probability of observing a value of loss greater than x, given that collapse has occurred, multiplied by the probability of observing collapse at a given intensity level. Component $P(L > x|NC, R) \cdot P(NC|E = e) \cdot P(R|NC, E = e)$ denotes the probability of observing a value of loss greater than x, given that no collapse has occurred and residual drifts deem the building irreparable, multiplied by the probability of observing no collapse at a given intensity level, multiplied by the probability of residual drifts rendering the building irreparable given no collapse has occurred. Lastly, component $P(L > x|NC, NR) \cdot P(NC|E = e) \cdot P(NR|NC, E = e)$ denotes the probability of observing a value of loss greater than x, given that no collapse has occurred and residual drifts do not deem the building irreparable, multiplied by the probability of observing no collapse at a given intensity level and the probability of residual drifts not rendering the building irreparable given no collapse has occurred. The integral shown in Equation 3 can be solved through numerical integration over the intensity levels considered in the assessment, where intensity e_i is assumed to represent all earthquake ground motion shaking intensities in the interval Δe_i.

The probabilities of observing no collapse and the probability of residual drifts rendering the building irreparable at the intensity levels considered in the assessment are shown in Table 2. The probabilities of observing no collapse were derived from the collapse fragility whereas the probabilities of residual drift rendering the building irreparable were obtained from the PACT analysis results, as discussed earlier.

Table 2. Probability of no collapse (PNC) and probability of residual drift rendering the building irreparable given no collapse (PR|NC) for the earthquake intensities considered.

Earthquake Ground Motion Intensity	PNC	PR|NC
e_1	0.021	1.000
e_2	0.057	1.000
e_3	0.148	1.000
e_4	0.341	1.000
e_5	0.647	0.319
e_6	0.921	0.068
e_7	0.998	0.004
e_8	1.000	0.000

Total building replacement cost was assumed in the event of collapse occurring. Similarly, if residual drifts deem the building irreparable the building was assumed at total loss. At those intensity levels considered in the assessment where low probabilities of collapse are observed, a loss curve was developed with PACT, which provides the probability of non-exceedance for a certain value of loss. Observed realizations follow a lognormal distribution as shown in Figures 5a through 5d. Due to the small number of realizations not triggering collapse for intensity levels e_1 to e_4, there is difficulty in developing accurate estimates of loss given no collapse. For these cases it was assumed that permanent deformations in the structure would deem the building irreparable as noted in Table 2. The resulting loss function

for the archetype building is shown in Figure 6a. Given the loss function, expected AAL can be calculated per Equation 4 (Jayaram et al. 2012):

$$AAL = \sum_{i=1}^{N} \Delta\lambda_i \cdot L_i \quad (4)$$

Where N in the number of intensity levels considered in the assessment, $\Delta\lambda_i$ is the annual rate of occurrence of intensity level i, as denoted in Figure 1, and L_i is the expected loss at intensity level i. The AAL for the archetype building is estimated at \$0.6M or 0.46% of building replacement cost. In addition to the AAL, loss exceedance rates can also be computed per Equation 5 (Jayaram et al. 2012):

$$ER(x) = 1 - e^{-\sum_{i=1}^{N} \Delta\lambda_i \cdot P(L>x)} \quad (5)$$

The exceedance rates for 10%, 20% and 40% of building replacement cost, or \$13.5M, \$27M and \$54M respectively, are 95, 208 and 524 years respectively.

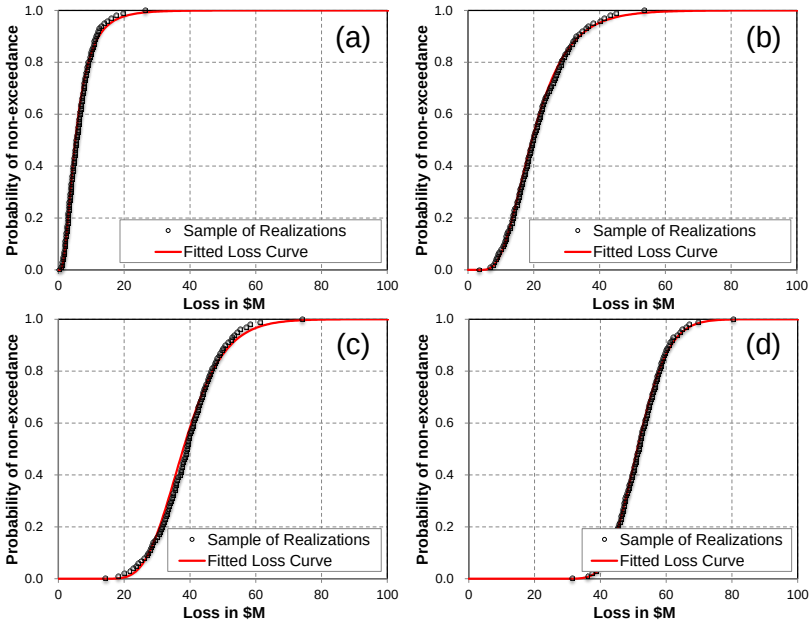

Figure 5. Sample loss realizations and fitted loss curves for earthquake ground motion intensities e_8 (a), e_7 (b), e_6 (c), e_5 (d).

Decision Making

In order to influence decision making, direct economic losses were selected as the metric to communicate performance in this study. Additionally, the annual rate of $\lambda_{Collapse}$ was used to benchmark the performance of the archetype tall building against the annual rates of collapse inherent to current building codes. The annual rate of collapse of the archetype building is estimated at 0.0015. The intent in current building codes is to produce designs with a 10 percent chance of collapse with shaking at the maximum considered earthquake level and earlier provisions suggest a design intent of less than one percent change of collapse in a 50 year period (FEMA 2009). If we assume that collapse occurrence follows a Poisson process, based on the annual rate of collapse, the probability of collapse for the archetype existing tall building in a 50 year period was estimated at 7%, which is roughly seven times the risk implied for new buildings. Under a the maximum considered earthquake (MCE) level for San Francisco, which has a characteristic return period of about 1000 years, the probability of collapse is 55%, which is over five times the probability implied for new buildings. At a ground motion with a 2475 year return period, or 0.0004 AFE, the expected SA at the fundamental period of the structure is 0.24g and the corresponding probability of collapse is 93%. These

metrics indicate that the collapse probability of the archetype existing tall building is significantly higher than that intended in current building codes. Short of collapse, the risk of non-repairable damage due to excessive drifts are even larger. Typically, residual drifts in the 0.25% to 0.5% require realignment of the structural frame and related structural repairs and residual drifts in the 0.5% to 1% range require major structural realignment to restore margin of safety for lateral stability though the level of repair may not be economically feasible (FEMA 2012). Apart from the life-safety implications, these high collapse and demolition risks can have enormous consequences on communities.

Similar to the probability of collapse in a period of time, the loss curve provides the expected losses for a given return period. For instance, a $14.5M loss (11% of the building replacement value) has a return period of 100 years or a $53M loss (39% replacement value) has a return period of 500 years, as shown in Figure 6a. The expected AAL is a useful metric to determine insurance premiums. The AAL for the archetype tall building is estimated at is $0.6M or 0.46% of building replacement cost. Furthermore, the AAL can be used to conduct cost benefit analyses of adopting structural retrofit or other building enhancements. Cost-benefit analyses conduct a comparison between the net present value of the average annual costs that are prevented through enhanced seismic performance. The net present value of an array of equal annual avoided expenditures is given by Equation 6 (FEMA 2012, Thuesen and Fabrycky 1984):

$$NPV = AAL \cdot \left\{ \frac{1-\frac{1}{(1+i)^t}}{i} \right\} \tag{6}$$

Where NPV is the net present value, AAL is the average annual loss previously defined, t is the time in years and i represents the interest rate. This approach enables cost-benefit analysis for different retrofit strategies. For example, if we assume a $3M investment aimed at enhancing the seismic performance of the building yields a 30% reduction in the AAL, the return on investment will take place in 10 years, given a 5% interest rate, as illustrated in Figure 6b.

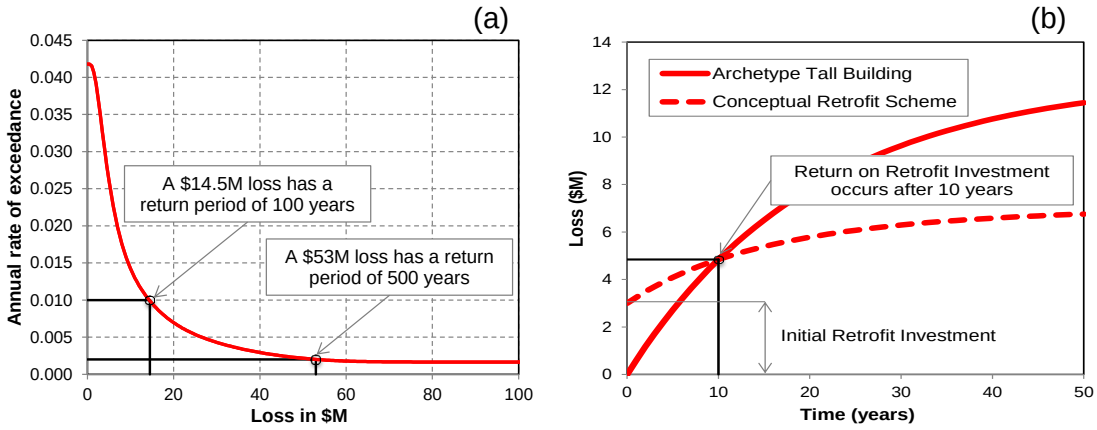

Figure 6. Loss function for archetype building (a) and cost-benefit analysis methodology (b).

CONCLUSIONS AND FUTURE WORK

This study presents the results of a risk-based seismic performance assessment of an archetype tall building representative of the existing tall buildings in San Francisco, CA. The collapse risk of the archetype building is considerably larger (about 5 to 7 times larger) that the intent of current seismic design codes. The loss assessment indicates the potential for substantial losses in the building, with annualized losses on the order of 0.5% of the building value and an expected loss in 100 years equal to about 11% of the building value. The study also highlights how the information presented can be used to inform decision about enhancing the seismic behaviour of the building, whether through structural retrofit or non-structural enhancements. Future studies will implement the proposed methodology to conduct cost-benefit analysis of different retrofit strategies.

REFERENCES

ASCE (2010). “Minimum design loads for buildings and other structures.” ASCE/SEI 7-10, American Society of Civil Engineers, Reston, VA.

Baker, J. W. (2015). “Efficient analytical fragility function fitting using dynamic structural analysis.” Earthquake Spectra, (in press).

NEHRP (2011). “Selecting and scaling earthquake ground motions for performing response-history analyses.” NIST GCR 11-917-15 prepared by NEHRP Consultants Joint Venture for the National Institute of Standards and Technology, Gaithersburg, MD.

FEMA (2006). “Next generation performance based seismic design guidelines. Program plan for new and existing buildings.” FEMA 445, Prepared by the Applied Technology Council for the Federal Emergency Management Agency, Washington, D.C.

FEMA (2009). “NEHRP recommended seismic provisions for new buildings and other structures.” FEMA P-750 Report, Federal Emergency Management Agency, Washington, D.C.

FEMA (2012). “Seismic performance assessment of buildings.” FEMA P-58, Prepared by the Applied Technology Council for the Federal Emergency Management Agency, Washington, D.C.

Goulet ,C., Haselton, C., Mitrani-Reiser, J., Beck, J., Deierlein, G., Porter, K. and Stewart, J. (2007). “Evaluation of the seismic performance of a code-conforming reinforced-concrete frame building from seismic hazard to collapse safety and economic losses.” Earthquake Engng. Struct. Dyn., 36:1973–1997.

Ibarra, L. and Krawinkler, H. (2005). “Global collapse of frame structures under seismic excitation.” Dept. of Civil and Environmental Engineering, Stanford University. Report No. 152, Stanford, CA.

Jayaram, N., Shome, N. and Rahnama, M. (2012). Development of earthquake vulnerability functions for tall buildings.” Earthquake Engng. Struct. Dyn., 41: 1495–1514.

Krawinkler, H. and Miranda, E. (2004). “Performance-Based Earthquake Engineering.” In: Bozorgnia Y. and Bertero V., Earthquake Engineering: From Engineering Seismology to Performance-Based Engineering, CRC Press, Chapter 9.

LS-DYNA (2013). Livermore Software Technology Corporation (LSTC) Version 971.

Medina, R. and Krawinkler, H. (2003). “Seismic Demands for non-deteriorating frame structures and their dependence on ground motions.” Dept. of Civil and Environmental Engineering, Stanford University. Report No. 144, Stanford, CA.

Moehle, J. and Deierlein, G. (2004). “A framework methodology for performance-based earthquake engineering.” Proc., 13th World Conference of Earthquake Engineering, Vancouver, B.C., Canada.

Molina Hutt, C. (2013). "Non-Linear Time History Analysis of Tall Steel Moment Frame Buildings in LS-DYNA." Proc., 9th European LS-DYNA Conference, Manchester, UK.

Molina Hutt, C., Almufti, I., Willford, M., Deierlein, G. (2014). “Seismic Loss and Downtime Assessment of Existing Tall Steel-Framed Buildings and Strategies for Increased Resilience.” American Society of Civil Engineers, Journal of Structural Engineering, Special Issue: Resilience-based Design of Structures and Infrastructures (accepted).

PEER (2010). “Tall buildings initiative: guidelines for performance-based seismic design of tall buildings.” Pacific Earthquake Engineering Research Center, Report No. 2010/05, College of Engineering, University of California, Berkeley.

PEER (2013). “PEER NGA-West2 Database.” Pacific Earthquake Engineering Research Center, Report No. 2013/03, College of Engineering, University of California, Berkeley.

Thuesen, G. J. and Fabrycky, W. J. (1984). “Engineering Economy.” Prentice-Hall, ISBN: 013028128X.